

Moisture distribution in concrete subjected to rain induced wetting-drying

Kaustav Sarkar* and Bishwajit Bhattacharjee^a

Department of Civil Engineering, Indian Institute of Technology Delhi, Hauz Khas, New Delhi - 110016, India

(Received January 29, 2013, Revised July 13, 2014, Accepted July 23, 2014)

Abstract. A rational estimation of moisture distribution in structural concrete is vital for predicting the possible extent and rate of progression of impending degradation processes. The paper proposes a numerical scheme for analysing the evolution of moisture distribution in concrete subjected to wetting-drying exposure caused by intermittent periods of rainfall. The proposed paradigm is based on the stage wise implementation of non-linear finite element (FE) analysis, with each stage representing a distinct phase of a typical wet-dry cycle. The associated boundary conditions have been constituted to realize the influence of various meteorological elements such as rain, wind, relative humidity and temperature on the exposed concrete surface. The reliability of the developed scheme has been demonstrated through its application for the simulation of experimentally recorded moisture profiles reported in published literature. A sensitivity analysis has also been carried out to study the influence of critical material properties on simulated results. The proposed scheme is vital to the service life modelling of concrete structures in tropical climates which largely remain exposed to the action of alternating rains.

Keywords: concrete; wetting-drying; moisture distribution; FE analysis

1. Introduction

Degradation of concrete is largely a moisture dependent phenomenon. Most commonly, the state of unsaturation attained under the influence of general ambient conditions leads to the corrosion of embedded steel and subsequent failure of structural elements (Broomfield 2007). Thus, to reliably estimate the durability performance of structural concrete it is imperative to model its interaction with the meteorological elements of temperature, wind, relative humidity and rainfall which compositely constitute its service environment (Nilsson 1996). Relevance of such modelling pursuits is particularly critical for those exposure types which bear the potential to aggravate the rate and extent of the impending degradation. The severity of wetting-drying exposure in this context is well established and in a tropical climate its manifestation occurs in the form of intermittent rains. While rain induced wetting causes a conspicuous ingress of water resulting in the saturation of cover zone concrete, subsequent drying renders the medium unsaturated. A continual exposure to wetting-drying cycles results in the evolution of degradation

*Corresponding author, Research Scholar, E-mail: srkrkaustav@gmail.com

^aProfessor, Ph.D., E-mail: bishwa@civil.iitd.ac.in

processes (Schiessl 1988); the most pervasive being the carbonation of concrete leading to the subsequent corrosion of embedded reinforcement (Parrott 1990; Stewart *et al.* 2011; Talukdar and Banthia, 2013). Thus, to reliably assess the durability performance of concrete elements subjected to wetting-drying conditions, the investigation of associated moisture distribution becomes necessary. This aids in identifying the thickness of cover zone susceptible to carbonation and in ascertaining the possible rate of its progression.

The experimental determination of moisture distribution in general involves the measurement of local moisture content at a finite number of points distributed across the medium. Several techniques varying from the simple gravimetric analysis of specimen segments (Terrill *et al.* 1986; Selih *et al.* 1996) to more sophisticated methods such as the application of sensors (West and Holmes 2001; Yeo *et al.* 2006a, b; Norris *et al.* 2008), neutron radiography (de Beer *et al.* 2004; Zhang *et al.* 2011) and magnetic resonance imaging (Pel 1995; Cano-Barrita *et al.* 2004) have been implemented for the practical determination of moisture profiles. While the experimental works carried out over the years have extensively investigated the uniaxial drying of concrete under constant temperature and humidity conditions, the study of the effect of alternating wet and dry conditions has received only a little attention. In a pioneering effort, Andrade *et al.* (1999) studied the variation of average relative humidity and temperature within the cover zone of concrete samples exposed to natural rainfall. Lately, Ryu *et al.* (2011) have also reported observations on the evolution of humidity and saturation states at different depths in a concrete specimen subjected to artificially created rainfall and summertime conditions. In a recent study on wet-dry cycles, albeit not simulating a natural exposure condition, Zhang *et al.* (2012) have investigated the variation of pore humidity caused due to the action of ponding and subsequent drying of specimen surface. These studies have provided a valuable impetus to the understanding of the hygro-thermal behaviour of concrete under the action of wetting-drying cycles. However, the complexity of controlling several influencing factors and the imprecision involved in the indirect measurement of moisture render the choice of such experimental pursuits less lucrative. This in turn calls for the development of efficient mathematical models for the characterization of associated moisture transport. The approach facilitates examining the influence of critical parameters on the wetting and drying behaviour of the material without resorting to extensive experimental programmes.

Two distinct modelling approaches have been traditionally used in the study of moisture movement in concrete. The more elaborate of the two starts with the formulation of balance equations at the micro level and then uses volume averaging to yield the macroscopic description. The method though more complicated is particularly suitable for modelling the hygro-thermal behaviour of concrete at early ages (Gawin *et al.* 2006a) and for simulating the deformations occurring due to shrinkage and creep (Gawin *et al.* 2006b). The phenomenological approach on the other hand starts directly from the macroscopic level and lumps the effect of various influencing factors in a few model parameters which are to be determined experimentally. On account of the relative simplicity of this approach, several models to describe the transfer of moisture and heat in porous building materials have been developed on its basis. A number of studies are documented in literature, which employ the latter approach in conjunction with the finite element (FE) method to analyze the coupled flow of moisture, heat and carbon dioxide in concrete (Saetta *et al.* 1993, 1995; Isgor and Razaqpur 2004). These schemes primarily attempt to predict the propagation of concrete carbonation in relation to the pore humidity. But in the context of rain induced wetting, which involves capillary uptake of water, representation of the imbibed moisture in terms of degree of pore saturation becomes imperative. This also provides an

additional advantage due to its relevance in predicting the corrosion kinetics (Lopez and Gonzalez 1993; Andrade *et al.* 2002). However, an analysis in terms of pore saturation relies on the quantification of the saturation and the equilibrium moisture contents. Determining the latter under given conditions of temperature and relative humidity in turn relies on the quantitative description of the pore structure characteristics of concrete. Only a few numerical studies (Li *et al.* 2008a, 2008b) are available in literature which relate to the modelling of wetting-drying action and determination of associated moisture penetration depth in concrete. However, even these illustrations do not realistically perceive the influence of the ambient conditions on the porous matrix of concrete for determining the concomitant moisture distribution.

The present work proposes a comprehensive procedure for the determination of moisture distribution in concrete subjected to intermittent spells of rainfall. To rationally account for the varied exposure conditions constituting a typical wetting-drying cycle, the analysis has been delineated into stages, each corresponding to a distinct phase of the cycle. The moisture boundary conditions corresponding to the identified stages have been modelled by integrating the effect of dominant meteorological elements and their interaction with the exposed concrete surface, which in turn govern the distribution of moisture within the medium. Considering the flow of moisture in unsaturated medium to be governed by the Richard's equation, the scheme implements a non-linear FE analysis to determine the moisture distribution in terms of degree of saturation. The moisture content corresponding to the states of saturation and equilibrium under the given conditions have been suitably quantified in terms of pore structure characteristics. The novelty of the present work is thus in realistically reckoning the synergy of ambient conditions constituted by the elements of rain, wind, relative humidity, temperature and the porous matrix of concrete for evaluating the evolution of moisture distribution under the influence of intermittent rains. The scheme however neglects any possible alteration of the microstructure due to the short term effects of carbonation and leaching. It also ignores the moisture movement occurring due to osmotic effects caused by high concentration of solutes in pore water and the negligible contribution of convective moisture transport occurring under the existence of temperature gradients in the medium.

The scheme has been implemented for a concrete medium subjected to one dimensional wetting and drying conditions reported by Ryu *et al.* (2011) to demonstrate its reliability. For this purpose a computer program has been developed in this work which simulates the evolution of moisture distribution. A sensitivity analysis has also been carried out to identify the influence of the vital material properties on the simulated results.

2. Description of wetting-drying cycle

Wetting-drying of RC structures in tropical climates is typically caused due to the occurrence of intermittent spells of rainfall. Wetting commences with the incidence of rain flux on the exposed concrete surface, initiating the ingress of moisture under an unsaturated surface condition. The duration of this phase depends on the intensity of the impinging rain flux and on the hydraulic diffusivity of concrete. After the attainment of surface saturation, wetting occurs with only a fraction of the incident flux forming the capillary uptake and the rest constitutes a run off (Hall and Kalimeris 1982). Drying on the other hand occurs in the period interim between two consecutive rainfall events. Similar to other inorganic materials, the drying of concrete can be considered to occur in distinct stages, differing primarily in the evolution of their rates of drying (Hall *et al.* 1984; Toei 1996). Initially, the loss of moisture occurs at a constant rate dependent on the ambient

conditions of temperature, relative humidity and wind speed. This period of constant rate drying lasts until the availability of free moisture on the exposed concrete surface. Subsequently, as the quantity of moisture within the capillary pores gradually reduces and gets segmented, the associated flow becomes progressively sluggish and the rate of drying falls accordingly. Thus, the moisture distribution analysis associated with a typical wetting-drying cycle can be delineated into the following four stages - (i) wetting under flux boundary condition; (ii) wetting under saturated surface condition; (iii) drying with a constant rate; (iv) drying with a falling rate. Since the porous matrix of concrete remains unsaturated under the influence of intermittent rains, the study of associated moisture distribution relies on the modelling of unsaturated flow under the influence of appropriate boundary conditions.

The phenomenon of moisture flow in an unsaturated porous medium is conventionally represented using the extended Darcy's law, stated as, $\partial\theta/\partial t = \nabla(D(\theta)\nabla\theta)$. For a one dimensional domain, the governing equation reduces to,

$$\frac{\partial\theta}{\partial t} = \frac{\partial}{\partial x} \left(D(\theta) \frac{\partial\theta}{\partial x} \right) \quad (1)$$

with the term, $D(\theta)\partial\theta/\partial x$ representing a flux acting in the direction of outward normal to the surface of the domain.

Here, θ (m^3/m^3) is the moisture content, t (s) is the time variable, x (m) is the space variable and $D(\theta)$ (m^2/s) is the moisture dependent hydraulic diffusivity function.

3. Modified model for unsaturated flow

Since the constituting parameters, viz. the hydraulic diffusivity of concrete, moisture content, the space and time variables differ by several orders of magnitude, it is advantageous to express Eq. (1) in terms of scaled parameters for the sake of computational efficiency. The scaled, non-dimensional parameters adopted in the present work are, (i) Reduced moisture content: $\theta_r = (\theta - \theta_o) / (\theta_s - \theta_o)$; (ii) Reduced distance: $x_r = V_o x / D_{d_wet}$ and (iii) Reduced time: $t_r = V_o^2 t / D_{d_wet}$

where, θ_o (m^3/m^3) is the moisture content of totally dry concrete, θ_s (m^3/m^3) is the free saturation moisture content of concrete, D_{d_wet} (m^2/s) is the wetting diffusivity of totally dry concrete and V_o ($\text{m}^3/\text{m}^2\text{s}$) is the rain flux.

Substituting the following partial derivatives determined using the stated relations for reduced parameters,

$$\frac{\partial\theta}{\partial t} = \frac{V_o^2 (\theta_s - \theta_o)}{D_{d_wet}} \cdot \frac{\partial\theta_r}{\partial t_r}; \quad \frac{\partial\theta}{\partial x} = \frac{V_o (\theta_s - \theta_o)}{D_{d_wet}} \cdot \frac{\partial\theta_r}{\partial x_r}; \quad \frac{\partial^2\theta}{\partial x^2} = \frac{V_o^2 (\theta_s - \theta_o)}{D_{d_wet}^2} \cdot \frac{\partial^2\theta_r}{\partial x_r^2}$$

Eq. (1) can be reframed as,

$$\frac{\partial \theta_r}{\partial t_r} = \frac{1}{D_{d_wet}} \frac{\partial D_r(\theta_r)}{\partial \theta_r} \left(\frac{\partial \theta_r}{\partial x_r} \right)^2 + \frac{D_r(\theta_r)}{D_{d_wet}} \frac{\partial^2 \theta_r}{\partial x_r^2} \quad (2)$$

with, $V_o(\theta_s - \theta_o)D_r(\theta_r)/D_{d_wet} \cdot \partial \theta_r / \partial x_r$ as the corresponding boundary flux in the direction of outward normal to the surface.

In Eq. (2), $D(\theta_r)$ (m²/s) is the diffusivity function in terms of reduced moisture content. Now, if for the phase of wetting, $D(\theta_r) = D_{d_wet} f_w(\theta_r)$ where, $f_w(\theta_r)$ is a function of reduced moisture content such that $f_w(\theta_r = 0) = 1$, then Eq. (2) reduces to,

$$\frac{\partial \theta_r}{\partial t_r} = \frac{\partial f_w(\theta_r)}{\partial \theta_r} \left(\frac{\partial \theta_r}{\partial x_r} \right)^2 + f_w(\theta_r) \frac{\partial^2 \theta_r}{\partial x_r^2} \quad (3)$$

with the following boundary conditions for the two encompassed stages,

During stage (i), a rain flux V_o (m³/m²s) remains incident on the exposed surface, thus,

$$V_o(\theta_s - \theta_o) \frac{D_r(\theta_r)}{D_{d_wet}} \frac{\partial \theta_r}{\partial x_r} = -V_o, \text{ at } x_r = 0$$

$$\text{i.e., } f_w(\theta_r) \frac{\partial \theta_r}{\partial x_r} = -\frac{1}{\theta_s - \theta_o}, \text{ at } x_r = 0 \quad (3a)$$

During stage (ii), the exposed surface maintains moisture content of θ_s (m³/m³), thus,

$$\theta_r = (\theta_s - \theta_o) / (\theta_s - \theta_o), \text{ at } x_r = 0$$

$$\text{i.e., } \theta_r = 1 \text{ at } x_r = 0 \quad (3b)$$

Similarly, if for the phase of drying, $D(\theta_r) = D_{w_dry} f_d(\theta_r)$ where, D_{w_dry} (m²/s) is the drying diffusivity of totally wet concrete and $f_d(\theta_r)$ is a function of reduced moisture content such that $f_d(\theta_r = 1) = 1$ then Eq. (2) can be modified as,

$$\frac{\partial \theta_r}{\partial t_r} = \frac{D_{w_dry}}{D_{d_wet}} \frac{\partial f_d(\theta_r)}{\partial \theta_r} \left(\frac{\partial \theta_r}{\partial x_r} \right)^2 + \frac{D_{w_dry}}{D_{d_wet}} f_d(\theta_r) \frac{\partial^2 \theta_r}{\partial x_r^2} \quad (4)$$

with the following boundary conditions at the exposed face,

During stage (iii), the evaporation of moisture from surface creates a mass flux J_c (kg/m²s), thus,

$$\frac{D_{w_dry}}{D_{d_wet}} f_d(\theta_r) \frac{\partial \theta_r}{\partial x_r} = \frac{(J_c / \rho_w)}{V_o(\theta_s - \theta_o)}, \text{ at } x_r = 0 \quad (4a)$$

where, ρ_w ($= 1000 \text{ kg/m}^3$) is the density of water.

During stage (iv), the exposed concrete surface attains an equilibrium moisture content θ_{eq} (m^3/m^3) under the influence of prevailing temperature and humidity conditions, thus,

$$\theta_r = (\theta_{eq} - \theta_0) / (\theta_s - \theta_0), \text{ at } x_r = 0 \quad (4b)$$

Eqs.(3) and (4) along with the associated boundary conditions in Eqs.(3a)-(3b) and Eqs.(4a)-(4b) govern the unsaturated flow problem corresponding to the phases of wetting and drying respectively. An investigation of Eqs.(3) and (4) reveals their inherent non-linearity owing to the presence of the moisture dependent functions $f_w(\theta_r)$ and $f_d(\theta_r)$.

3.1 Diffusivity functions

The distribution of moisture in a concrete medium is characterized by the nature of diffusivity function. The function is known to assume typical trends for the phases of wetting and drying respectively and the fact has been accounted for in the constitution of Eqs.(3) and (4). The sequel describes the established forms of the generic functions $f_w(\theta_r)$ and $f_d(\theta_r)$ referred to in the previous section.

The absorption of rain water in concrete is primarily caused due to the action of capillary forces. In this context, diffusivity describes the tendency of the material to transmit fluid by capillarity (Hall and Hoff, 2002). Thus, the term "diffusivity" borrowed due to the analogy of Eq. (1) with Fick's second law of diffusion if taken literally can be misleading (Hillel,1973). When the fluid being transmitted is water, diffusivity is specifically termed as the hydraulic diffusivity and is defined as the ratio of hydraulic conductivity to specific water capacity. The moisture sensitivity of these parameters renders diffusivity strongly dependent on moisture content. The hydraulic diffusivity governing the capillary uptake of water in a number of building materials has been successfully represented using an exponential function of the form (Lin 1992; Hall 1994; Pel 1995),

$$D_r(\theta_r) = D_{d_wet} \exp(n\theta_r) \quad (5a)$$

The value of n in the stated equation ranges between 6-8 for building materials (Hall 1989) and for concrete in an initially dry state a value of $n = 6$ has been suggested (Leech *et al.* 2003).

The phase of drying on the other hand involves moisture transport due to vapour diffusion, surface creep and liquid assisted vapour transport in addition to the bulk movement of liquid in partially and fully saturated pore spaces. The differences in the underlying mechanisms of moisture transport result in a separate functional form for drying diffusivity. The moisture dependency of drying diffusivity of concrete is represented using a 'S' shaped curve (Bazant and Najjar 1971, 1972),

$$D_r(\theta_r) = D_{w_dry} \left[\alpha_o + \frac{1 - \alpha_o}{1 + \left(\frac{1 - \theta_r}{1 - \theta_c} \right)^{n^*}} \right] \quad (5b)$$

with α_o representing the ratio of minimum to maximum drying diffusivity and the parameters θ_c and n^* characterizing the location of drop and the spread of the curve respectively. Lately, the experimental investigation performed by Wong *et al.* (2001) has also testified to the validity of this relationship.

The strong dependence of hydraulic diffusivity on moisture content renders the unsaturated flow problem highly non-linear. A plausible analysis of the problem therefore demands the application of a robust numerical scheme which has been discussed in the following section.

4. FE formulation

The present work implements the FE method to address the inherent non-linearity of the moisture transport problem under study. The FE model for the time dependent problem has been developed using decoupled formulation where time and space variations are assumed to be separable (Reddy 2005). The formulation commences with the determination of the weak form of the governing differential equation using the weighted residual approach. For the phase of wetting governed by Eq. (3), the weak form of the governing equation is given by,

$$\int_0^l w_j \left(\frac{\partial \theta_r}{\partial t_r} \right) dx_r + \int_0^l f_w(\theta_r) \frac{\partial w_k}{\partial x_r} \frac{\partial \theta_r}{\partial x_r} dx_r = w_j f_w(\theta_r) \frac{\partial \theta_r}{\partial x_r} \Big|_0^l \quad (6)$$

The variable θ_r in Eq. (6) is approximated as, $\theta_r(x_r, t_r) = \sum_{j=1}^m N_j(x_r) \theta_{rj}(t_r)$ and following the Galerkin's method (Reddy 2005) the weight terms can be substituted with interpolation functions, i.e. $w_j = N_j$ ($j=1$ to m). Now, for a two noded ($m=2$) linear element,

$$\theta_r = \left[\left(1 - \frac{x_r}{l} \right) \left(\frac{x_r}{l} \right) \right] \begin{Bmatrix} \theta_{r_1} \\ \theta_{r_2} \end{Bmatrix} = [N_1 \ N_2] \{d^e\} = [H] \{d^e\} \quad (6a)$$

$$\text{Thus, } \frac{\partial \theta_r}{\partial x_r} = \begin{bmatrix} -1 & +1 \\ l & l \end{bmatrix} \begin{Bmatrix} \theta_{r_1} \\ \theta_{r_2} \end{Bmatrix} = [B] \{d^e\} \quad (6b)$$

Here, l is the reduced length of the element, m is the number of nodes in the element, w_j is the weight function, θ_{r_1} and θ_{r_2} are the values of reduced moisture at nodes, $\{d^e\}$ is the vector of nodal values of reduced moisture, N_1 and N_2 are the interpolation functions for a two noded element, $[H]$ is the interpolation matrix and $[B]$ is the gradient matrix.

Thus, for $w_1 = N_1$ and $w_2 = N_2$ Eq. (6) yields,

$$\left[\frac{l}{3} \ \frac{l}{6} \right] \frac{\partial \{d^e\}}{\partial t_r} + f_w(\theta_r) \begin{bmatrix} +1 & -1 \\ l & l \end{bmatrix} \{d^e\} = - \left(f_w(\theta_r) \frac{\partial \theta_r}{\partial x_r} \right)_{x_r=0} \quad (6c)$$

$$\left[\frac{l}{6} \quad \frac{l}{3} \right] \frac{\partial \{d\}}{\partial t} + f(\theta) \left[\frac{-1}{l} \quad \frac{+1}{l} \right] \{d\} = \left(f(\theta) \frac{\partial \theta}{\partial x} \right)_r \quad (6d)$$

Combining Eqs.6(c) and 6(d), the element level governing equation for the phase of wetting can be obtained as,

$$\frac{l}{6} \begin{bmatrix} 2 & 1 \\ 1 & 2 \end{bmatrix} \frac{\partial \{d^e\}}{\partial t_r} + \frac{f_w(\theta_r)}{l} \begin{bmatrix} +1 & -1 \\ -1 & +1 \end{bmatrix} \{d^e\} = \left\{ \begin{array}{l} - \left((f_w(\theta_r)) \frac{\partial \theta_r}{\partial x_r} \right)_{x_r=0} \\ + \left((f_w(\theta_r)) \frac{\partial \theta_r}{\partial x_r} \right)_{x_r=l} \end{array} \right\} \quad (6e)$$

Similarly, for the phase of drying,

$$\frac{l}{6} \begin{bmatrix} 2 & 1 \\ 1 & 2 \end{bmatrix} \frac{\partial \{d^e\}}{\partial t_r} + \frac{D_{w_dry}}{D_{d_wet}} \frac{f_d(\theta_r)}{l} \begin{bmatrix} +1 & -1 \\ -1 & +1 \end{bmatrix} \{d^e\} = \left\{ \begin{array}{l} - \frac{D_{w_dry}}{D_{d_wet}} \left((f_d(\theta_r)) \frac{\partial \theta_r}{\partial x_r} \right)_{x_r=0} \\ + \frac{D_{w_dry}}{D_{d_wet}} \left((f_d(\theta_r)) \frac{\partial \theta_r}{\partial x_r} \right)_{x_r=l} \end{array} \right\} \quad (6f)$$

Eq. 6(e) and Eq. 6(f) represent a set of ordinary differential equations in the form, $[m]\{\dot{d}^e\} + [k]\{d^e\} = \{q\}$, where $[m]$ and $[k]$ are referred to as the element level mass and diffusivity matrices, $\{\dot{d}^e\}$ is the vector of time derivatives of nodal degrees of freedom and $\{q\}$ is the vector of nodal fluxes. The time derivatives contained in the semi discrete system of equations when substituted using suitable finite difference approximations provide a completely discretized system of equations. Thus by implementing the Crank-Nicolson scheme a set of algebraic equations can be obtained as,

$$\left([m] + \frac{\Delta t_r}{2} [k]^{n+1} \right) \{d^e\}^{n+1} = \left([m] - \frac{\Delta t_r}{2} [k]^n \right) \{d^e\}^n + \frac{\Delta t_r}{2} (\{q\}^{n+1} + \{q\}^n) \quad (6g)$$

With a given set of initial values, the nodal values of reduced moisture at the end of $(n+1)^{th}$ time step is determined through the iterative solution of the above equation using global mass and diffusivity matrices.

Ju and Kung (1997) have demonstrated that the use of lumped mass scheme with linear elements provides stable convergence and consistent results for FE based solution of Richard's equation and the same scheme has been adopted in the present study. Furthermore, a fine mesh with a reduced element length of $l=0.5$ and a small value of Δt_r incrementing in the range of $[1 \times 10^{-5}, l^2)$ is effective for reliably capturing the evolution of moisture profile in the highly non-linear problem.

5. Modelling of moisture conditions at boundary

The evolution of moisture distribution in a concrete medium subjected to intermittent rainfall occurs under the influence of a fluctuating state of moisture at the exposed surface. The realistic modelling of these moisture states has to account for the interaction of the meteorological elements with the material in relation to its hygro-thermal properties. The sequel describes the models adopted in the present scheme to represent the relevant boundary conditions and duly emphasizes the underlying assumptions wherever relevant.

5.1 Rain flux

The joint occurrence of wind and rain causes an oblique rain intensity vector which is referred to as the wind driven rain (WDR) (Blocken and Carmeliet 2004). In the context of interaction between rain and vertical facade of a structure, the term WDR intensity refers to the component of rain intensity vector acting perpendicular to the vertical surface as shown in Fig. 1.

A semi empirical method is most commonly used to calculate the WDR intensity using commonly available meteorological data and is given by the expression after Lacy (1977),

$$V_o = 0.222WR^{0.88} \quad (7)$$

where, V_o (mm/h) is the WDR intensity, W (m/s) is the wind speed and R (mm/h) is the rainfall intensity.

It is however to be noted that since the measurement of rainfall intensity and wind speed are done in an undisturbed air stream, Eq. (7) does not account for the effects induced by local topography and the geometry of the structure itself. A better estimate of WDR intensity can be obtained by following the provisions of ISO 15927-3:2009 which provides a procedure to analyze hourly weather data incorporating the effects of local terrain, topography, obstacles and wall geometry.

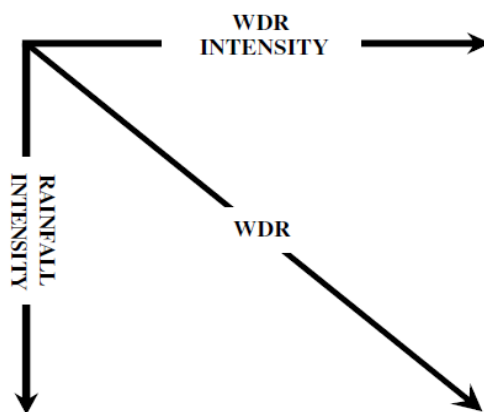


Fig. 1 Components of Wind Driven Rain

5.2 Saturation moisture content

The total porosity of concrete is primarily constituted by spaces separating the gel masses formed around the partially hydrated cement grains and by the pores contained within the gel itself. The former component of porosity is referred to as the capillary porosity and it predominantly provides for the movement of moisture in concrete. The pores in gel which constitute the gel porosity however offer only a minor passageway to water due to their very small size. The fraction of total porosity of concrete available for the transport of fluids is generally referred to as its open porosity (Hall and Hoff 2002). However, the saturation caused by free capillary uptake of water would fill up only a fraction of the open pore space. In the dearth of any reliable model for the estimation of pore volume which remains open to free saturation, the proposed scheme considers it to be equal to the capillary porosity. Following the Power's model, the capillary porosity of concrete can be approximated using the relation (Neville and Brooks 1987),

$$\phi_c = \frac{\frac{w}{c} - 0.36h + \frac{a}{C}}{0.317 + \frac{A_f}{\rho_f C} + \frac{A_c}{\rho_c C} + \frac{w}{c} + \frac{a}{C}} \quad (8)$$

Thus, in the proposed scheme, $\theta_s = \phi_c$. Here, ϕ_c (m^3/m^3) is the capillary porosity of concrete, h is the degree of hydration of cement, w/c is the water to cement ratio by mass, a (m^3/m^3) is the volume of entrapped air in concrete, C , A_f and A_c are the parts of cement, fine and coarse aggregates by mass, ρ_f and ρ_c are the specific gravities of fine and coarse aggregate respectively.

Apart from the conventional specification of mix proportions and other ancillary data, Eq. (8) incorporates the degree of hydration of cement as an input parameter. The latter can be determined for a given curing age t_{cure} (in days) by employing the following empirical expression after Kondraivendhan and Bhattacharjee (2010),

$$h = C_1 \cdot \ln(w/c) + C_2 \cdot \ln(t_{cure}) + C_3 \quad (8a)$$

Using experimental data from literature in conjunction with laboratory results, the values of the constant coefficients in the stated equation have been estimated for OPC 43 (IS 12269:1989) grade cement by Kondraivendhan (2010) as, $C_1 = 0.217$, $C_2 = 0.07$ and $C_3 = 0.591$ for curing carried out at room temperature.

5.3 Evaporation flux

During the initial stage of drying, the exposed facade of the element attains wet bulb temperature due to evaporative cooling. For the given ambient conditions of temperature T_a ($^{\circ}\text{K}$) and relative humidity RH , the wet bulb temperature T ($^{\circ}\text{K}$) can be estimated with sufficient accuracy by iteratively solving the following equation proposed by Oteh (1985) for psychrometric calculations,

$$p_w = \exp(14.481133 - 5333.3/T_w) - 6.66 \times 10^{-4} p_b (T_a - T_w) \quad (9)$$

with the parameter on the left hand side being evaluated using the relation, $p_w = RH \cdot p_s$ where,

$$p_s = \exp(14.481133 - 5333.3/T_a) \quad (9a)$$

Here, p_w (bar) is the vapour pressure of water in air, p_s (bar) is the saturated vapour pressure of air and $p_b = 1.013$ (bar) is the barometric/atmospheric pressure.

The difference of temperature which prevails between the wet concrete surface and the ambient air causes a convective flow of heat towards the surface causing evaporation of moisture and resulting in a concomitant flux given by,

$$J_c = (h_f / \gamma_{w,T=T_w}) \cdot (T_a - T_w) \quad (10)$$

where, h_f (W/m²K) is the film heat transfer coefficient and $\gamma_{w,T=T_w}$ (J/kg) is latent heat of vaporization of water at T °K.

For a given temperature difference, the parameters $\gamma_{w,T}$ and h_f in Eq. (10) regulate the quantity of flux generated. An estimate of $\gamma_{w,T}$ at any temperature T °K can be obtained by using the Watson's expression (Smith *et al.* 2005),

$$\gamma_{w,T} = 2257 \times 10^3 \left(\frac{1 - (T/T_c)}{1 - (373.15/T_c)} \right)^{0.38} \quad (10a)$$

where, $T_c = 647.1^\circ \text{K}$ is the critical temperature of water.

The equation expresses $\gamma_{w,T}$ as a function of reduced temperature i.e. (T/T_c) and estimates the same using its known value at some other temperature. In Eq. (10a), 2257×10^3 J/kg is the latent heat of vaporization of water at 373.15 °K. The empirical equation is widely accepted due to its simplicity and fair accuracy.

A gross empirical estimate of h_f can be obtained for a windward surface if the free stream wind speed W (m/s) is known by using the relationship (Palyvos 2008),

$$h_f = 7.4 + 4.0W \quad (10b)$$

5.4 Equilibrium moisture content

The evaporative loss of water from a porous solid subjected to constant conditions of temperature and relative humidity, gradually leads to a state of equilibrium in moisture transport. At equilibrium, only a fraction of the pore volume constituted by pores of size lesser than a threshold value r_{eq} (nm) remains saturated due to capillary condensation and the rest remains unsaturated with only a thin layer of adsorbed water molecules covering the pore surface area

(Espinosa and Franke 2006; Ishida *et al.* 2007). The equilibrium moisture content can thus be expressed as,

$$\theta_{eq} = V_s + V_u \quad (11)$$

where, V_s (m^3/m^3) is the volume of water in saturated pores and V_u (m^3/m^3) is the volume of water contained in the unsaturated pores of concrete. The term V_s in Eq. (11) in fact corresponds to the cumulative volume of pores with size lesser than and equal to r_{eq} in a unit volume of concrete, while V_u can be defined as, $V_u = At_a$ where, A is the cumulative surface area of pores with size greater than r_{eq} in a unit volume of concrete and t_a (nm) is the thickness of the adsorbed moisture layer.

To estimate the threshold pore size delineating the saturated and unsaturated pore volumes, the Kelvin's radius r_k (nm), representing the maximum pore radius amenable to capillary condensation can be taken as the basis and is given by (Hall and Hoff, 2002),

$$r_k = \frac{-2 \times 10^9 V_m \sigma}{\bar{R} T_a \log(RH)} \quad (12)$$

where, $V_m = 18 \times 10^{-6}$ (m^3/mol) molar volume of water, σ (N/m) surface tension of water and $\bar{R} = 8.314$ (J/mol.K) is the universal gas constant.

The surface tension of water in Eq. (12) can be well represented over a wide range of temperature using the following empirical relation (Lyklema 2000),

$$\sigma = 0.2358 \left(1 - \frac{T}{T_c}\right)^{1.256} \left[1 - 0.625 \left(1 - \frac{T}{T_c}\right)\right] \quad (12a)$$

To further incorporate the influence of ink bottle pores which result in the retention of moisture in pores of size greater than r_k during drying, the concept of form factor (f^*) after Espinosa and Franke (2006) has been implemented. Accounting for the thickness of adsorbed moisture layer and the ink bottle effect, the threshold value of pore size can be determined as, $r_{eq} = f^* \times (r_k + t_a)$ and shall be referred to as the equilibrium radius in this work. The thickness of the adsorbed moisture layer can be satisfactorily estimated using the empirical expression (Espinosa and Franke 2006; Thomas *et al.* 1999),

$$t_a = 0.395 - 0.189 \ln(-\ln(RH)) \quad (13)$$

Adopting $f^* = 3$, which has been previously demonstrated by Espinosa and Franke (2006) to provide a satisfactory description of capillary drying, the equilibrium moisture content of concrete can be determined using Eq. (11). Evidently, the determination of θ_{eq} relies on the quantification of cumulative volume and surface area of pores as a function of the pore radius. The variation of cumulative pore volume $V_{at r}$ (m^3/m^3) with pore entry radius r (nm) has been successfully represented by Patil and Bhattacharjee (2008) using the relation,

$$V_{at\ r} = \phi_c r_{0.5}^d / (r^d + r_{0.5}^d) \quad (14)$$

Here, $V_{at\ r}$ corresponds to the volume of all pores of size greater than and equal to r . The associated parameters, $r_{0.5}$ (nm) and d represent the median pore size corresponding to 50% cumulative pore volume and the dispersion coefficient respectively. For ASTM type-I cement these parameters can be determined using the following empirical equations (Kondraivendhan 2010),

$$r_{0.5} = (24.79/t_{cure}) + 71.87(w/c) + 0.865 \quad (14a)$$

$$d = 1.14(w/c) - 0.644 \ln(w/c) + 0.214 \ln(t_{cure}) - 0.778 \quad (14b)$$

The relationship in Eq. (14) has been reported to hold good for a wide range of construction materials including concrete. Thus, under the previously stated assumption $\theta_s = \phi_c$, the quantity of water in saturated pores can be calculated using Eq. (14) as,

$$V_s = \phi_c - V_{at\ r=r_{eq}} \quad (15)$$

The determination of moisture contained in unsaturated pores on the other hand depends on the estimation of the corresponding cumulative surface area. An expression for cumulative surface area of pores is given by,

$$A = \frac{1}{\gamma |\cos \phi|} \int_0^V p dV \quad (16)$$

where, A is the cumulative surface area of pores constituting a volume V , γ is the surface tension of penetrating fluid, p is capillary pressure and ϕ is the contact angle in degrees.

From Washburn's equation it is known that,

$$p = -2\gamma \cos \phi / r \quad (16a)$$

And from Eq. (14),

$$r = r_{0.5} [(\phi_c - V) / V]^{1/d} \quad (16b)$$

Substituting Eqs. (16a) and (16b) in Eq. (16), A (nm^2/nm^3) can be expressed as,

$$A = \frac{2}{r_{0.5}} \int_0^V V^{1/d} (\phi_c - V)^{-1/d} dV \quad (16c)$$

The integral in Eq. (16c) can be numerically evaluated between the limits 0 to $V_{at\ r=r_{eq}}$ and having determined A , the moisture content of unsaturated pores can be calculated as, $V_u = At_a$.

6. Scheme implementation

The previous section has elaborated the models used in the present scheme for the simulation of moisture boundary conditions corresponding to the different phases of wetting-drying cycle. These models primarily rely on conventional mix proportion data and on the specification of temperature-humidity conditions as inputs. Taking these inputs from the experimental study of Ryu *et al.* (2011), the developed scheme has been implemented using a computer program to simulate the reported evolution of moisture profiles recorded with the aid of sensors embedded at depths of 10mm, 30 mm, 50 mm, 70 mm and 90 mm from the exposed surface of a specimen of 100 mm depth and subjected to one dimensional wetting and drying conditions. As per the investigation of Ryu *et al.* (2011), the present analysis has considered a series of exposure scenarios starting with (i) 45 days of drying under constant temperature (20°C) and humidity (60%), followed by (ii) 4 days of drying under constant temperature (20°C) and changing humidity (57 - 89.7%), followed by (iii) 4 days of drying under constant humidity (60%) and changing temperature (21.9 - 28.3°C), followed by (iv) 4 days of drying with changing humidity (57 - 89.7%) and changing temperature (21.9 - 28.3°C) and finally (v) 1 day of wetting under an artificially simulated rainfall of 30.1 mm/h intensity. After Ryu *et al.* (2011), the temperature has been taken to vary diurnally attaining peak in 16 hours starting from its minimum and falling back to minimum in 8 hours; humidity has been considered to alter on the same time frame but in an opposite sense.

The material properties and mix proportion data reported by Ryu *et al.* (2011) which serve as inputs to the present analysis are furnished in Table 1 for reference. Furthermore, an equivalent curing period at 20°C corresponding to the accelerated curing regime of 30 days at 60°C followed by 10 days at 20°C adopted by Ryu *et al.* (2011) has been determined using the rule of maturity (Neville and Brooks 1987),

$$(T_{cure} - T_{ref}) \times t_{cure} = t_1 (T_1 - T_{ref}) + t_2 (T_2 - T_{ref}) \quad (17)$$

where, $T_{ref} = -11^\circ\text{C}$ is the reference temperature below which the strength development ceases, $T_{cure} = 20^\circ\text{C}$, $T_1 = 60^\circ\text{C}$, $T_2 = 20^\circ\text{C}$, $t_1 = 30$ days, $t_2 = 10$ days and t_{cure} is the equivalent curing period in days. Substitution of the stated values in Eq. (17) gives $t_{cure} = 79$ days.

In addition to these inputs, the simulation of moisture distribution requires the specification of parameters which constitute the wetting and drying diffusivity functions. As has been demonstrated by Wong *et al.* (2001), for a given concrete these parameters are to be determined through extensive experimentation. Since these parameters have not been reported by Ryu *et al.* (2011), their values have been suitably assumed with reference to the data available in published literature. The parameters in the drying diffusivity function have been reported to assume identical values for drying temperatures beyond 20°C and the reported values $\alpha_o = 0.025$, $\theta_c = 0.792$ and $n^* = 6$ (Hanson 1968; Wong *et al.* 2001) have been adopted.

The parameter n in the wetting diffusivity function has been reported to assume a value of 6 for an initially dry concrete medium. Adopting this value would therefore provide a higher estimation of water penetration depth in a medium which is initially in a partially saturated state (Leech *et al.* 2003). Thus, to account for the weakening of capillary action caused due to the initial condition of partial saturation the value of $n = 6$ has been reduced by a fraction $(1 - \theta_{r,av})$ where, $\theta_{r,av}$ (m^3/m^3) is the average reduced moisture content of the medium prior to the initiation of moisture ingress. The adopted approach is in conformance to the experimental observation relating the reduction in sorptivity to the initial moisture content of the concrete medium (Hall 1989; Wong *et al.* 2001).

Table1 Mix proportion data

w/c	Slump (mm)	Air (%)	Water (kg/m ³)	Cement (kg/m ³)	Fine Agg. (kg/m ³)	Coarse Agg. (kg/m ³)
0.60	145	3.7	170	283	825	1035
	Specific Gravity:-			3.16	2.59	2.65

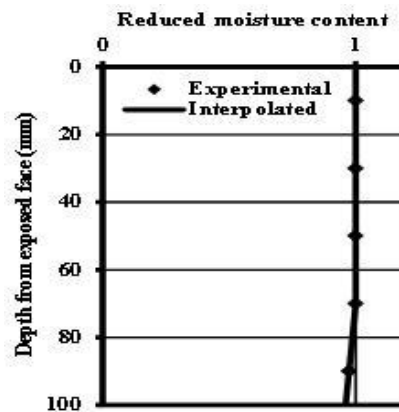


Fig. 2 Initial moisture distribution – profile constituted using experimental data

In the present analysis, a value of $\theta_{r,av} = 0.647$ has been adopted on the basis of the initial moisture profile reported by Ryu *et al.* (2011) and thus the value of $n = 2.12$.

The values of $D_{d,wet}$ and $D_{w,dry}$ have been determined through trial and error to achieve a reasonable match of the simulated moisture profile with the first reported profile observed after 5 days of drying at 20°C and 60% RH; the values of $D_{d,wet} = 14.96 \times 10^{-10} \text{ m}^2/\text{s}$ and $D_{w,dry} = 14.14 \times 10^{-10} \text{ m}^2/\text{s}$ result in an average absolute percentage difference of 3.67%. It has been described in the following paragraphs that, extending the simulation further using these values provides a consistent match of the predicted results with the reported profiles corresponding to the various exposure conditions stated earlier and this testifies to the correctness of the adopted values. To further investigate the influence of the values of these parameters on the variability of simulated results a sensitivity analysis has been carried out and the obtained results have been presented in the following section.

Constituting the initial moisture profile (Fig. 2) on the basis of the experimental data reported by Ryu *et al.* (2011), the analysis has been initiated with exposure condition (i) stated earlier. Fig.3 presents a comparison of the predicted moisture profiles with available experimental results obtained after every 5 days of drying. As depicted in the figure using error bars, the predicted results can be seen to lie within a range of $\pm 10\%$ of experimental values, while the computed average absolute percentage difference is 5.4%. Under the given exposure condition, the constant rate drying period has been found to prevail for 3948 s and only the surface node attained equilibrium thereafter during the rest of the drying period.

The simulation has been sequentially extended further for exposure conditions (ii), (iii) and (iv) and a comparison of the experimental data with predicted profiles is presented in Figs. 4(a)-4(c) respectively. Similar to the results obtained for constant temperature-humidity conditions, the predicted values for dynamic exposure conditions also lie within a range of $\pm 10\%$ of the reported

experimental values with an average absolute percentage difference of 5.6%, 6.0% and 6.1% respectively for the corresponding scenarios.

In the next phase, the effect of exposure condition (v) on the state of moisture distribution in an initially unsaturated concrete specimen has been analysed. As in (Ryu *et al.* 2011), for this particular phase, the moisture profile obtained at the end of the previous exposure scenario has not been taken to be the initial condition. As shown in Fig. 5, it has instead been constituted using

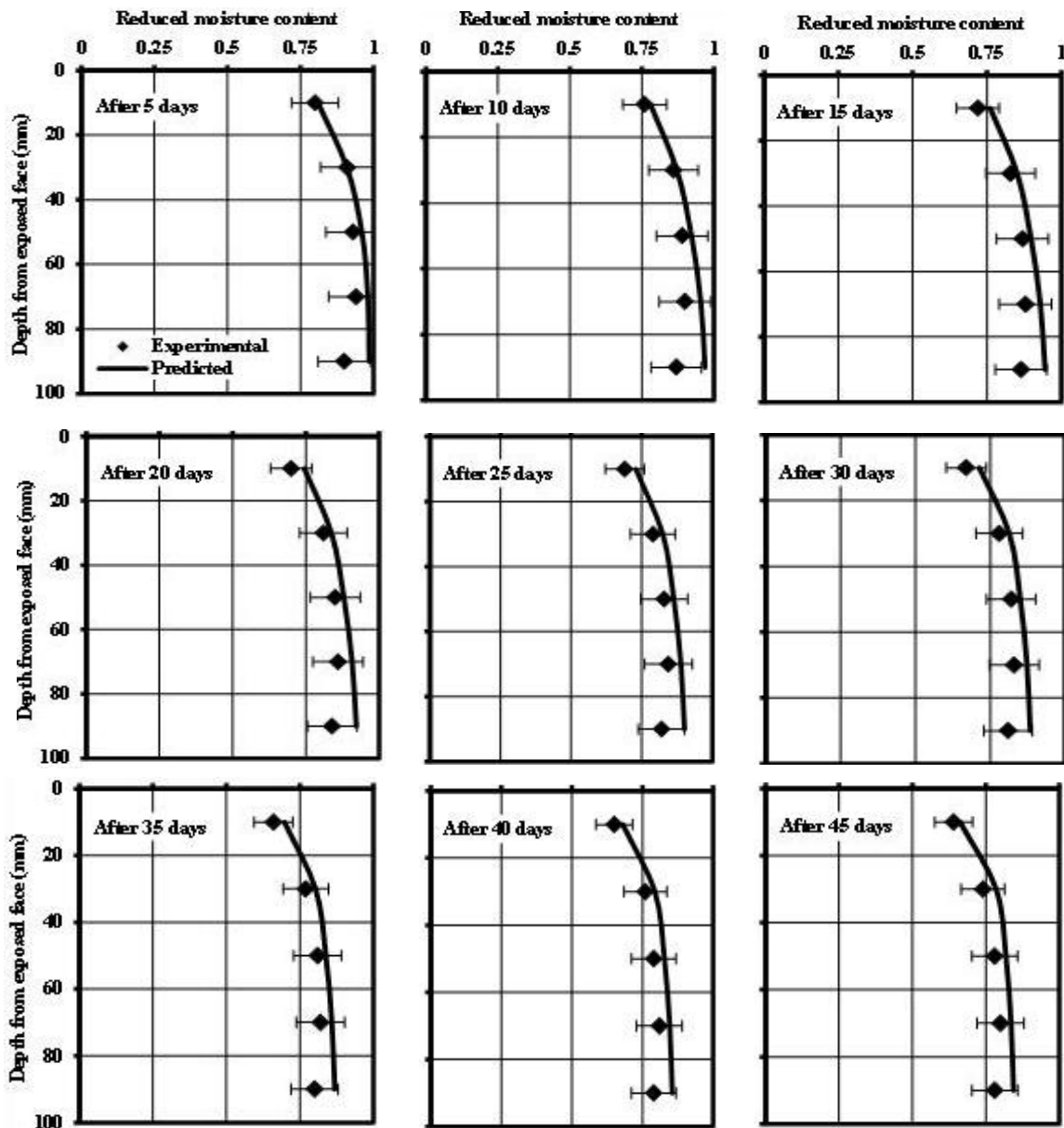


Fig. 3 Evolution of moisture distribution due to one dimensional drying at 20°C and 60% humidity

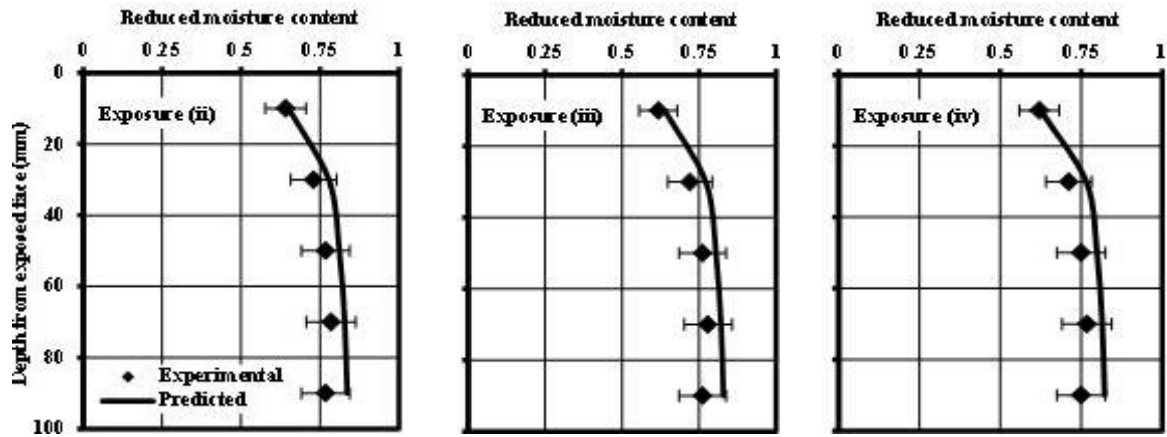


Fig. 4 Moisture distribution resulting after (a) exposure (ii); (b) exposure (iii); (c) exposure (iv)

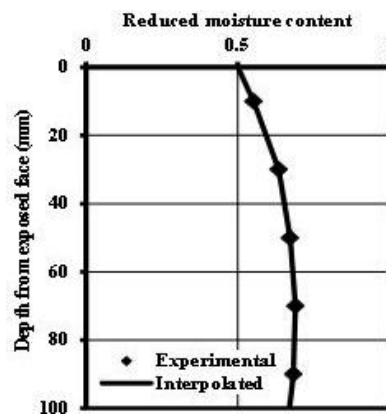


Fig. 5 Moisture distribution in the specimen prior to its exposure to artificial rain – profile constituted using experimental data

the explicitly specified discrete values of reduced moisture at depths of 10 mm, 30 mm, 50 mm, 70 mm and 90 mm. Also, the reported values have been averaged to obtain an estimate for the diffusivity function parameter $\theta_{r,av}$ stated earlier. Under the given test conditions, the results of analysis indicated an instantaneous attainment of surface saturation. Figs. 5(b)-5(d) compare the simulated evolution of moisture content at depths of 10 mm, 30 mm and 50 mm with the reported experimental observations during the 24 hour exposure period. Except for the predicted moisture evolution at 30 mm depth which deviates beyond 10% of experimental data, the simulations at depths of 10mm and 50 mm are in good agreement with reported data. The average absolute percentage difference between the predicted and experimental observations is 5.0%. It is evident from Figs. 6(a)-6(c) that the predicted moisture penetration is significant only up to a depth of 30 mm from the exposed surface and this fact is in conformation with the observations reported by Ryu *et al.* (2011).

For all the exposure conditions considered, the average variation of simulated results in relation

to the reported experimental data lies in the range of 5-6%. The accuracy of the sensor used for the measurement of humidity in the study of Ryu *et al.* (2011) has been reported to be $\pm 1.5\%$ and further perceiving the possibility of calibration and experimental errors, the simulated observations can be considered to be reliable.

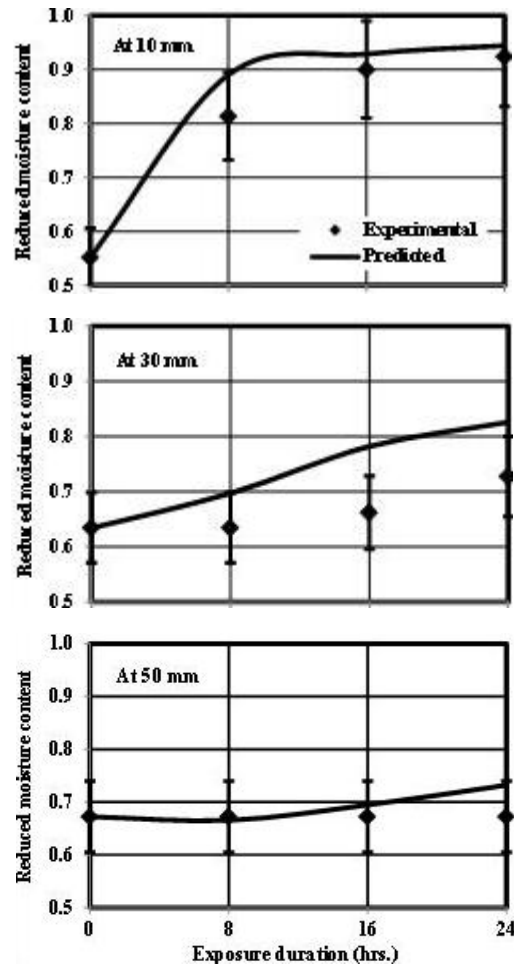


Fig. 6 Evolution of moisture content at depths of (a) 10 mm; (b) 30 mm; (c) 50 mm, from the exposed surface of specimen subjected to rain

Table 2 Sensitivity of simulated moisture distribution to $D_{w,dry}$ (keeping $D_{d,wet} = 14.96 \times 10^{-10} \text{ m}^2/\text{s}$)

$D_{w,dry}$ (m^2/s)	Average absolute percentage difference w.r.t. experimental data				
	Exposure(i)	Exposure(ii)	Exposure(iii)	Exposure(iv)	Exposure(v)
11.31×10^{-10}	7.4	8.7	9.3	9.5	5.0
12.73×10^{-10}	6.4	7.1	7.6	8.0	5.0
14.14×10^{-10}	5.4	5.6	6.0	6.1	5.0
15.55×10^{-10}	4.4	4.8	4.5	5.6	5.0
16.97×10^{-10}	3.7	4.5	4.3	5.4	5.0

Table 3 Sensitivity of simulated moisture distribution to D_{d_wet} (keeping $D_{w_dry} = 14.14 \times 10^{-10} \text{ m}^2/\text{s}$)

D_{d_wet} (m^2/s)	Average absolute percentage difference w.r.t. experimental data				
	Exposure(i)	Exposure(ii)	Exposure(iii)	Exposure(iv)	Exposure(v)
11.97×10^{-10}	5.4	5.6	6.0	6.1	3.7
13.46×10^{-10}	5.4	5.6	6.0	6.1	4.4
14.96×10^{-10}	5.4	5.6	6.0	6.1	5.0
16.45×10^{-10}	5.4	5.6	6.0	6.1	5.6
17.95×10^{-10}	5.8	5.7	6.1	6.2	6.1

6.1 Sensitivity analysis

The illustration in the previous section adopted the values for diffusivity function parameters D_{d_wet} and D_{w_dry} using a trial and error procedure. It is thus pertinent that any imprecision in the estimation of these values would affect the quality of simulated results. To evaluate the extent of influence of these parameters a sensitivity analysis has been carried out by linearly varying the two parameters within 0.8 to 1.2 times of the adopted values in steps of 0.1 and the observed sensitivity of results to D_{w_dry} and D_{d_wet} are furnished in Tables 2 and 3 respectively.

It can be seen in Table 2 that increasing values of D_{w_dry} result in a decrease in the average absolute percentage difference of the simulated and experimental results for all the drying scenarios i.e. exposure (i)-(iv). On an average, an increase of 10% and 20% reduces the difference by 5.2% and 22.5% respectively. On the other hand, the data in Table 3 reveals that decreasing the value of D_{d_wet} produces better results for the wetting scenario i.e exposure (v). Reducing the value of D_{d_wet} by 10% and 20% offsets the difference by 12% and 26% respectively. On the basis of these findings it can thus be concluded that the parameters D_{d_wet} and D_{w_dry} can have a very significant effect on the nature of simulated moisture profiles. It is thus necessary to develop reliable models for the estimation of these parameters to facilitate a robust analysis of moisture transport phenomena and associated durability performance of structural concrete.

7. Summary and conclusions

A mathematical framework for the phenomenon of rain induced wetting-drying has been proposed and a numerical procedure has been developed for predicting the concomitant evolution of moisture distribution in concrete. To achieve computational efficiency, a set of non-dimensional parameters has been used to constitute a modified form of Richard's equation governing the unsaturated flow phenomena. A time dependent, non-linear finite element model has been formulated to facilitate a robust analysis of the highly nonlinear problem. Analysis of moisture transport under the proposed scheme is carried out in four separate stages, each corresponding to a distinct state of moisture condition on the exposed concrete surface. The boundary conditions for the identified stages have been modelled rationally by taking into account the influence of dominant meteorological elements on the porous matrix of concrete.

By adopting suitable values for the diffusivity function parameters, the developed scheme has been implemented using a computer program to simulate experimentally measured moisture profiles reported in published literature. The satisfactory agreement of experimental and predicted moisture profiles testify to the reliability of the developed procedure in determining the state of

moisture distribution in concrete subjected to wetting-drying exposure. It can however be perceived that the model may not provide correct estimates in cases where a high temperature gradient prevails in the medium. Moreover, as reflected in the sensitivity analysis, the significant influence of diffusivity values for concrete has been established. The developed procedure is an effective tool for the determination of moisture distribution in concrete for appropriate modelling of degradation processes, especially in the context of service life prediction of RC structures in tropics where rain induced wetting-drying is a common phenomenon.

References

- Andrade, C., Alonso, C. and Sarria, J. (2002), "Corrosion rate evaluation in concrete structures exposed to atmosphere", *Cement Concrete Comp.*, **24**(1), 55-64.
- Andrade, C., Sarria, J. and Alonso, C. (1999), "Relative humidity in the interior of concrete exposed to natural and artificial weathering", *Cement Concrete Res.*, **29**(8), 1249-1259.
- Schiessl, P. (1988), *Corrosion of steel in concrete*, Report of the technical committee 60-CSC RILEM, Chapman and Hall, London and New York.
- Bazant, Z.P. and Najjar, L.J. (1972), "Nonlinear water diffusion in non saturated concrete", *Mater. Struct.*, **5**(1), 3-20.
- Bazant, Z.P. and Najjar, L.J. (1971), "Drying of concrete as a non linear diffusion problem", *Cement Concrete Res.*, **1**(5), 461-473.
- Blocken, B. and Carmeliet, C. (2004), "A review of rain driven wind research in building science", *J. Wind Eng Ind. Aerod.*, **92**(13), 1079-1130.
- Broomfield, J.P. (2007), *Corrosion of steel in concrete: understanding, investigation and repair. 2nd ed.*, Taylor & Francis, London, England and New York, USA.
- Cano-Barrita, P.F.de.J., Balcom, B.J., Bremner, T.W., MacMillan, M.B. and Langley, W.S. (2004), "Moisture distribution in drying ordinary and high performance concrete cured in a simulated hot dry climate", *Mater. Struct.*, **37**(8), 522-531.
- de Beer, F.C., Strydom, W.J. and Griesel, E.J. (2004), "The drying process of concrete: a neutron radiography study", *Appl. Radiat. Isotopes*, **61**(4), 617-623.
- Espinosa, R.M. and Franke, L. (2006), "Inkbottle pore-method: prediction of hygroscopic water content in hardened cement paste at variable climatic conditions", *Cement Concrete Res.*, **36** (10), 1954-1968.
- Gawin, D., Pesavento, F. and Schrefler, B.A. (2006a), "Hygro-thermo-chemo-mechanical modelling of concrete at early ages and beyond. Part I: Hydration and hygro-thermal phenomena", *Int. J. Numer. Meth. Eng.*, **67**(3), 299-331.
- Gawin, D., Pesavento, F. and Schrefler, B.A. (2006b), "Hygro-thermo-chemo-mechanical modelling of concrete at early ages and beyond. Part II: Shrinkage and Creep of Concrete", *Int. J. Numer. Meth. Eng.*, **67**(3), 332-363.
- Hall, C. (1994), "Barrier performance of concrete: a review of fluid transport theory", *Mater. Struct.*, **27** (5), 291-306.
- Hall, C. (1989), "Water sorptivity of mortars and concretes: a review", *Mag. Concrete Res.*, **41** (147), 51-61.
- Hall, C. & Hoff, W.D. (2002), *Water transport in brick, stone and concrete*, Taylor & Francis, London, England and New York, USA.
- Hall, C. and Kalimeris, A.N. (1982), "Water movement in porous building materials - V. Absorption and shedding of rain by building surfaces", *Build. Environ.*, **17**(4), 257-262.
- Hall, C., Hoff, W.D. and Nixon, M.R. (1984), "Water movement in porous building materials - VI. Evaporation and drying in brick and block materials", *Build. Environ.*, **19** (1), 13-20.
- Hanson, J.A. (1968), "Effects of curing and drying environments on splitting tensile strength", *ACI Mater. J.*, **65**(7), 535-543.
- Hillel, D. (1973), *Soil and Water - Physical Principles and Processes*, Academic Press, New York, USA and

- London, England.
- IS 8112 (1989), *Specification for 43 Grade Ordinary Portland Cement*, Bureau of Indian Standards, New Delhi, India.
- Isgor, O.B. and Razaqpur, A.G. (2004), "Finite element modeling of coupled heat transfer, moisture transport and carbonation processes in concrete structures", *Cement Concrete Comp.*, **26** (1), 57-73.
- Ishida, T., Maekawa, K. and Kishi, T. (2007), "Enhanced modelling of moisture equilibrium and transport in cementitious materials under arbitrary temperature and relative humidity history", *Cement Concrete Res.*, **37** (4), 565-578.
- ISO 15927-3 (2009), *Hydrothermal performance of buildings – Calculation and presentation of climatic data - Part 3*, Calculation of a driving rain index for vertical surfaces from hourly wind and rain data. DIN, Germany.
- Ju, S.H. and Kung, K.J.S. (1997), "Mass types, element orders and solution schemes for the Richard's equation", *Comput. Geosci.*, **23**(2), 175-187.
- Kondraivebdhan, B. and Bhattacharjee, B. (2010), "Effect of age and water-cement ratio on size dispersion of pores in ordinary portland cement paste", *ACI Mater. J.*, **107** (2), 147-154.
- Kondraivendhan, B. (2010), "Influence of w/c ratio and age on pore size distribution of OPC and fly ash pastes and mortars", Ph.D. Dissertation, Indian Institute of Technology Delhi, New Delhi.
- Lacy, R.E. (1977), *Climate and building in Britain*, HMSO, London.
- Leech, C., Lockington, D. and Dux, P. (2003), "Unsaturated diffusivity functions for concrete derived from NMR images", *Mater. Struct.* **36** (6), 413-418.
- Li, C., Li, K. and Chen, Z. (2008a), "Numerical analysis of moisture influential depth in concrete and its application in durability design", *Tsinghua Science and Technology*, **13**(1), 7-12.
- Li, C., Li, K. and Chen, Z. (2008b), "Numerical analysis of moisture influential depth in concrete during drying-wetting cycles", *Tsinghua Sci. Technol.*, **13**(5), 696-701.
- Lin, S.H. (1992), "Nonlinear water diffusion in unsaturated porous solid materials", *Int. J. Engng. Sci.*, **30** (12), 1677-1682.
- Lopez, W. and Gonzalez, J.A. (1993), "Influence of the degree of pore saturation on the resistivity of concrete and the corrosion rate of steel reinforcement", *Cement Concrete Res.*, **23** (2), 368-376.
- Lyklema, J. (1991), *Fundamentals of Interface and Colloid Science: Liquid-Fluid Interfaces*, Academic Press, London, England.
- Neville, A.M. and Brooks, J.J. (1987), *Concrete Technology*, Pearson Education Ltd., New Delhi, Delhi, India.
- Nilsson, L. (1996), "Interaction between microclimate and concrete - a prerequisite for deterioration", *Const. Build. Mater.*, **10** (5), 301-308.
- Oteh, U.U. (1985), "Equations for psychrometric calculations", *Int. J. Refrig.*, **8**(2), 116-117.
- Palyvos, J.A. (2008), "A survey of wind convection coefficient relations for building envelope energy systems' modelling", *Appl. Therm. Eng.*, **28** (8-9), 801-808.
- Parrott, L.J. (1990), "Damage caused by carbonation of reinforced concrete", *Mater. Struct.*, **23** (3), 230-234.
- Patil, S.G. and Bhattacharjee, B. (2008), "Size and volume relationship of pore for construction materials", *J. Mater. Civil Eng.*, **20** (6), 410-418.
- Pel, L. (1995), "Moisture transport in porous building materials", Ph.D. Dissertation, Technische Universiteit Eindhoven, Netherlands.
- Reddy, J.N. (2005), *An Introduction to the Finite Element Method. 3rd ed.*, TMH, New Delhi, Delhi, India.
- Ryu, D.W., Ko, J.W. and Noguchi, T. (2011), "Effects of simulated environmental conditions on the internal relative humidity and relative moisture content distribution of exposed concrete", *Cement Concrete Comp.* **33** (1), 142-153.
- Saetta, A.V., Schrefler, B.A. and Vitaliani, R.V. (1993), "The carbonation of concrete and the mechanism of moisture, heat and carbon dioxide flow through porous materials", *Cement Concrete Res.*, **23** (4), 761-772.
- Saetta, A.V., Schrefler, B.A. and Vitaliani, R.V. (1995), "2-D model for carbonation and moisture/heat flow in porous materials", *Cement Concrete Res.*, **25** (8), 1703-1712.

- Selih, J., Sousa, A.C.M. and Bremner, T.W. (1996), "Moisture transport in initially fully saturated concrete during drying", *Transport Porous Med.*, **24** (1), 81-106.
- Smith, J.M., Van Ness H.C. and Abbott, M.M. (2005), *Introduction to Chemical Engineering Thermodynamics. 7th ed.*, TMH, New York, NY, USA.
- Terrill, J.M., Richardson, M. and Selby, A.R. (1986), "Non-linear moisture profiles and shrinkage in concrete members", *Mag. Concrete Res.*, **38** (137), 220-225.
- Thomas, J.J., Jennings, H.M. and Andrew, J.A. (1999), "The surface area of hardened cement paste as measured by various techniques", *Concrete Science Eng.*, **1**(1), 45-64.
- Toei, R. (1996), "Theoretical fundamentals of drying operation", *Dry. Technol.*, **14** (1), 1-194.
- West, R. and Holmes, N. (2001), "Experimental investigation of moisture migration in concrete", *Proceedings of the Colloquium on Concrete Research in Ireland*, NUI, Galway, September.
- Wong, S.F., Wee, T.H., Swaddinwudhipong, S. and Lee, S.L. (2001), "Study of water movement in concrete", *Mag. Concrete Res.* **53** (3), 205-220.
- Zhang, J., Gao, Y. and Han, Y. (2012), "Interior humidity of concrete under dry-wet cycles", *J. Mater. Civil Eng.*, **24**(3), 289-298.
- Yeo, T.L., Cox, M.A.C., Boswell, L.F., Sun, T. and Grattan, K.T.V. (2006a), "Optical fibre sensors for monitoring ingress of moisture in structural concrete", *Rev. Sci. Instrum.*, **77**(5), 055108-055108-7.
- Yeo, T.L., Cox, M.A.C., Boswell, L.F., Sun, T. and Grattan, K.T.V. (2006b), "Monitoring ingress of moisture in structural concrete using a novel optical-based sensor approach", *J. Phys. Conf. Ser.*, **45**(1), 186-192.
- Norris, A., Saafi, M. and Romine, P. (2008), "Temperature and moisture monitoring in concrete structures using embedded nanotechnology/microelectromechanical systems (MEMS) sensors", *Const. Build. Mater.*, **22**(2), 111-120.
- Zhang, P., Wittmann, F.H., Zhao, T., Lehmann, E.H. and Vontobel, P. (2011). "Neutron radiography, a powerful method to determine time-dependent moisture distributions in concrete", *Nucl. Eng. Des.*, **241**(12), 4758-4766.
- Stewart, M.G., Wang, X. and Nguyen, M.N. (2011), "Climate change impact and risks of concrete infrastructure deterioration", *Eng. Struct.*, **33**(4), 1326-1337.
- Talukdar, S. and Banthia, N. (2013), "Carbonation in concrete infrastructure in the context of global climate change: Development of a service lifespan model", *Const. Build. Mater.*, **40**(2013), 775-782.